Investigation of adaptive optical components for high power mode matching in gravitational wave detectors

Michelle Snider
Dept. of Physics, Smith College, Northampton MA
David Reitze
Dept. of Physics, University of Florida, Gainesville FL
2 August 2002

ABSTRACT

Thermal lensing causes problems in high power, high precision experiments like gravitational wave detectors. A possible solution lies in the development of an active compensation scheme for high-power mode matching. This paper presents two options that offer a range of focusing while maintaining beam quality, necessary for proper mode-matching. A theoretical modeling program was developed to investigate a positive thermal lens induced by a heating beam hitting a piece of absorptive Schott glass. The glass is heated, changing the optical path length seen by a reading beam of non-absorptive wavelength. The modal characteristics of this beam were evaluated, and it was found that this compensation scheme offers great potential in a range of induced focal lengths with little power loss to higher-order modes. A second investigation was performed experimentally, using a heating coil to induce a negative thermal lens on a cylindrical TGG crystal. Initial tests indicated that a lens was being produced; however, due to asymmetries in the heating of the crystal, further characteristics were unable to be determined.

1. INTRODUCTION

The Laser Interferometer Gravitational Wave Observatory (LIGO) represents a collaborative effort by many universities to search for Einstein's theorized gravitational waves. These waves are proposed to be created by large-scale astronomical phenomena, such as binary inspirals that no longer emit light and must radiate energy through another means. The current LIGO interferometric detectors use a 10 W laser in a combination Michelson interferometer with Fabry-Perot arm cavities. At the current strain sensitivity, LIGO will at most detect only one event per year; however, the second generation (Advanced LIGO) will utilize a 200 W laser in an effort to increase sensitivity by an order of magnitude. This higher laser power causes problems in many of the optical components, the most significant of which is thermal lensing. In order for Advanced LIGO to accurately detect gravity waves, the resulting modal distortions in the beam must be corrected.

In this paper, we consider two methods for improving the coupling of the laser beam into the Fabry-Perot arm cavities using adaptive optics based on thermal lensing. Under ordinary circumstances, thermal lensing is a deleterious effect that degrades coupling into an optical cavity. However, in special cases, one can use the thermal lens created by heating an optical component to improve the coupling. Several methods have been proposed to demonstrate an adaptive optical component based on thermal lensing. The first creates a positive lens using a laser heating source. A piece of Schott glass that is transparent to the wavelength of the main beam is used. A second laser of a wavelength absorbed by the

glass is directed coaxially and heats the center of the material. This creates a thermal lens, which then affects the main beam. The power of the heating laser is adjustable; thus, the induced lens is variable. We investigated this technique using a modeling simulation written in Matlab, which, given the initial parameters of the beams and of the material, outputs the characteristics of the reading beam after it passes through the induced lens. We can thus determine the appropriate initial conditions to obtain a variable lens that preserves beam quality.

Alternatively, a negative lens can be created using the "toaster" method. A cylindrical terbium gallium garnet (TGG) crystal is heated by a concentric loop of nichrome wire. This material has a high resistance and thus when a current is passed through it, and most of its energy is radiated as heat. The outer portion of the crystal is heated more than the core, and thus a small temperature gradient is created. The index of refraction is temperature-dependent, so the heated crystal behaves like a concave lens. Again, the current through the wire is adjustable; consequently, the properties of the induced lens are variable. This method was tested experimentally, with the crystal and heating coil inside a vacuum container as they will be in Advanced LIGO. The lensing effects on the beam and the resulting beam quality were evaluated.

2. BACKGROUND INFORMATION

2.1 OVERVIEW OF GAUSSIAN OPTICS

In order to understand how LIGO works, one must have a basic understanding of Gaussian optics. Normal optics assumes that a laser beam has a finite size and for most applications, this approximation causes negligible error. However, for high-precision experiments like LIGO, a more accurate description must be used. Gaussian optics describes the intensity of the beam as following a Gaussian curve. Thus the peak intensity is at the center, and although the intensity becomes negligible at a certain point, it never entirely disappears (Fig. 1a).

The beam can be described by several characteristics: the radius of the beam at a given point, the waist location, and the radius of curvature (Fig. 1b). The waist is defined as the smallest radius of the beam along its path. The radius of the beam at any location z can be described mathematically as [1]

$$w(z) = w_0\sqrt{1+(z/z_R)^2} \qquad (1)$$

where w_o is the waist and z_R is the Rayleigh range [1]

$$z_R = \pi w_o^{\,2} / \lambda\,. \qquad (2)$$

At the Rayleigh range, the radius of the beam is larger than the waist by a factor of the square root of two. The radius of curvature at any point z can be determined using this value [1]:

$$R(z) = z + z_R^{\,2} / z \quad . \tag{3}$$

Any two of these variables define a beam. However, a beam is typically described in one complex variable, denoted as *q*, which takes into account both the waist and the radius of curvature. It is defined as

$$\frac{1}{q(z)} \equiv \frac{1}{R(z)} - i\left(\frac{\lambda}{\pi w^2(z)}\right) \quad . \tag{4}$$

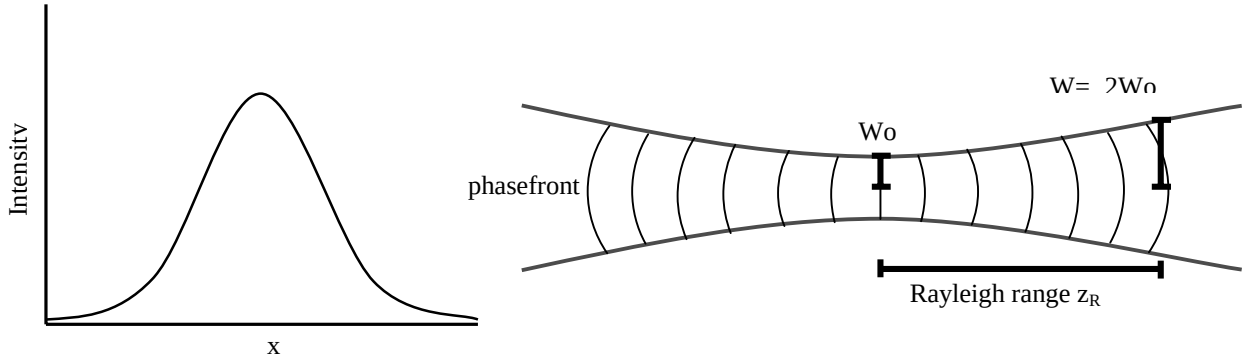

FIGURE 1: (a) Gaussian beam intensity (b) diagram showing waist, z_R

A crucial aspect of the LIGO experiment is the optical cavity. Created by placing two mirrors with specified radii of curvature facing each other, the cavity lets light in through the back of one mirror when on resonance, that is when the cavity length is an integer multiple of one-half wavelength of the entering light. The light then travels to the second mirror, reflects back, travels back to the first, reflects, etc. As light that is mode-matched to the cavity enters, it interferes constructively with the light already in the cavity, and the power contained in the cavity increases. After resonating within the cavity, light eventually exits through the second mirror. A photodiode placed after the cavity can be used to determine how much power is contained within.

Light will more efficiently enter the cavity if it is mode matched, meaning at the point of entry it has the same radius of curvature as the mirror. Light that is not mode-matched is reflected and does not enter the cavity. The radius of curvature of beam can be described as the sum of components, of light of a larger radius plus light of a smaller radius. Thus the component of the beam that has the same radius of curvature and waist location will enter the cavity, while the rest is back reflected. As the length of the cavity is changed, different components of light will make it in. These are called modes. By changing the length of the cavity, we can scan through all the different modes and determine how much power is in each.

Each beam can be described as a sum of any number of modes. The fundamental, or 00, mode is the perfect Gaussian beam, and appears in cross-section as a solid circle. Higher order modes are defined

in two categories, the circularly symmetric Leguerre-Gauss (LG) modes and the horizontally- and vertically-symmetric Hermite-Gauss (HG) modes. Several of the modes obtained in this experiment are shown in Figure 2.

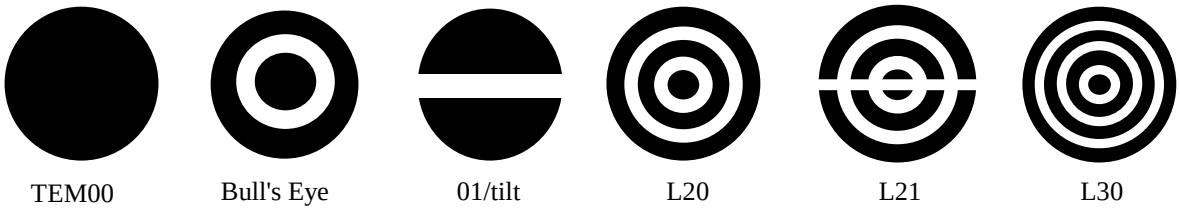

FIGURE 2: Common modes of the laser beam.

The different modes are indicative of different beam characteristics. For example, the LG10 mode is often referred to as the "tilt" mode, since it appears when the laser does not enter the cavity orthogonally. Another common mode is the "bull's eye" mode (BE), which is actually the sum of LG20 and LG02, and indicates that the laser is either wider or narrower than the 00 mode of the cavity.

2.2 THE LIGO PROJECT

The purpose of LIGO is to detect gravitational waves. The experimental setup is based on the Michelson interferometer, whereby an initial beam is split and directed down two arms. At the end of each arm is a mirror, which reflects the beam back in the direction from which it came. The two beams meet again at the original beam splitter, and depending on the difference in the lengths of the arms, constructively or destructively interfere (Fig. 3). The created light pattern is measured by a photodiode. The LIGO setup adapts this concept by adding Fabry-Perot optical cavities, in which the mode-matched beam will resonate. The lengths of the interferometric arms are such that the resonating beams will produce complete destructive interference. When a gravity wave passes by, one of the arms will become slightly longer, and the other will become slightly shorter. As the lengths of the cavities are changed, the beam will no longer be mode-matched and all the light will flood out. Light will then hit the photodetector in an interference pattern that will be used to determine by how much each arm length changed, and thus whether the event was actually a gravitational wave.

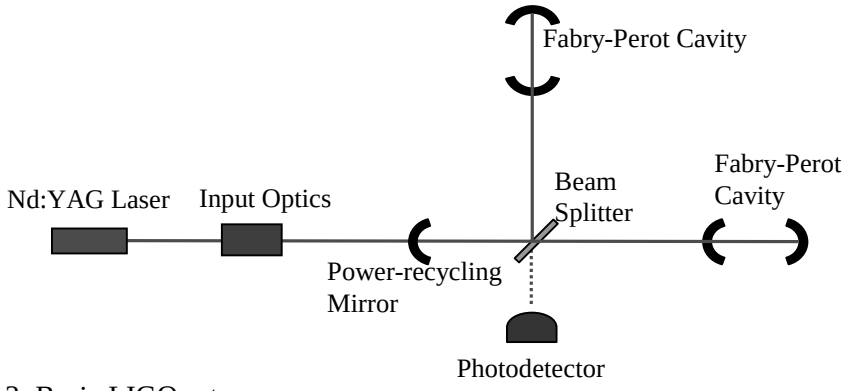

FIGURE 3: Basic LIGO setup.

Currently, the LIGO project is composed of three detectors. In Livingston, Louisiana, there is one interferometer with 4 km arms. In Hanford, Washington, there is another 4 km detector as well as a 2 km detector. Thus if a suspected gravity wave is detected at one site, it can be cross-checked against the other location. The two different sizes of detectors provide a second check, since the effects should be properly scaled. Each detector is composed of three main parts: the pre-stabilized laser (PSL), the input optics, and the core optics (the interferometer itself). The University of Florida (UF) is solely responsible for the input optics portion. The PSL is protected from back-reflections off the optical components, and the beam is cleaned and mode-matched before it enters the core optics. Additionally, a power-recycling mirror serves to reflect the light not directed into the photodetector back into the interferometer.

LIGO uses a 10 W, 1064 nm laser. In order to make it more sensitive and thus able to detect weaker signals, a second generation (Advanced LIGO) is being developed using a 200 W laser. Although the optical components in use are chosen for their extremely low levels of absorption, no material is completely transparent. At low laser power, the effects of this absorption, called thermal lensing, are negligible. However, at the power levels of Advanced LIGO, thermal effects cannot be ignored.

2.3 THERMAL LENSING

As laser light passes through an optical component, some of its energy is absorbed, the amount of which depends on the absorption coefficient of the material. The optical path length (OPL) seen by a beam changes due to three factors: thermal expansion of the material, photoelastic effect for isotropic materials, and change in the temperature-dependent index of refraction (dn/dT) [2]. For the LIGO project, we only consider the change in OPL (ΔOPL) due to the change in index of refraction, as the other two factors are negligible in comparison. This factor can be described mathematically as [2]

$$\Delta OPL = \frac{dn}{dT} L \Delta T(r) \tag{5}$$

where L is the length of the material, and T(r) is temperature as a function of radius. This can be found using the thermal diffusion equation [2]

$$\nabla^2 T(r) + \frac{q(r)}{k_{th}} = 0 \tag{6}$$

where q(r) is the heat source and k_{th} is the thermal conductivity of the material. Integration of this equation yields

$$\Delta T(r) = \frac{\alpha P}{4\pi k_{th}} \sum_{j=1}^{\infty} \frac{(-1)^j \left(\frac{2r^2}{w^2}\right)^j}{jj!} \tag{7}$$

where P is incident laser power, r is the radial location, and w is the radius of the incoming beam.

If dn/dT is positive, as in most materials, a positive (convex) lens will be created, and the beam will be focused. If dn/dT is negative, a negative (concave) lens will be created, and the beam will begin to diverge. In either case, the beam characteristics are changed and it will no longer be mode-matched. Thus in order for Advanced LIGO to properly detect gravity waves, these thermal distortions of the beam must be compensated. A possible solution lies in the development of an adaptive optical component for higher mode matching. Ideally this component would have a large range in focal length, while preserving the quality of the beam. I have investigated two possible methods, one theoretically and one experimentally.

3. THEORETICAL MODEL OF POSITIVE INDUCED THERMAL LENS

3.1 INTRODUCTION

We can use thermal lensing to our advantage by purposefully heating a material to induce a thermal lens. In theory we can create a lens which is variable and can thus be used to mode-match the beam. One method utilizes a material which is highly absorptive for certain wavelengths and transparent to others. A beam of one wavelength can be used to heat the material, which then expands and changes the optical path length (τ OPL) seen by a second beam of non-absorptive wavelength. In this model, we used Schott glass, which is highly absorptive in the visual range but not in the infrared. Thus, we chose a heating beam of wavelength 532 nm and a reading beam of wavelength 1064 nm. The profile of the created lens is Gaussian in shape. However, if the size of the reading beam is small enough to only pass through the circular tip of the curve, it will only see a perfect spherical convex lens and the quality of the beam can be maintained (Fig. 4).

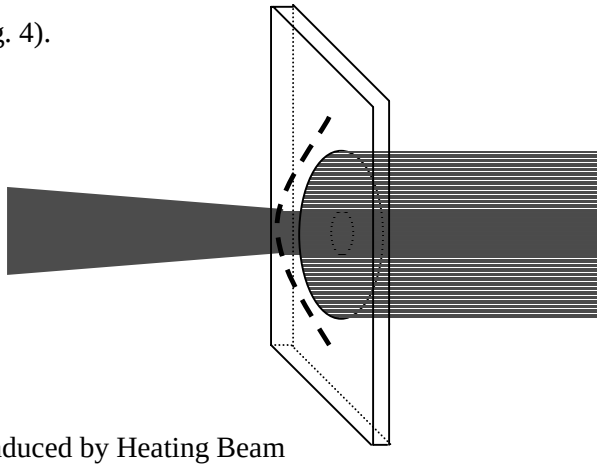

FIGURE 4: Thermal Lens Induced by Heating Beam

3.2 THEORETICAL BACKGROUND

The basis for the modeling program is modal aberration theory. When a beam passes through a material such as glass, the mode is changed depending on the ΔOPL at each point. In our case we will

assume that the incoming beam is a pure 00 mode Gaussian beam. This can be described by a radial intensity profile:

$$u_{00}(r) = \sqrt{\frac{2}{\pi}}\left(\frac{1}{w}\right)\exp\left(\frac{-r^2}{w^2}\right) \quad . \tag{8}$$

Here, w is the size of the beam and r is the distance from the waist. As the beam passes through the glass, the intensity profile is transformed into

$$u_{aber}(r) = u_{00}\exp\left(\frac{i2\pi\Delta OPL}{\lambda}\right) \quad . \tag{9}$$

where ΔOPL is computed using equations 4-6 using the writing beam as heat source, and τ is the wavelength of the light. The solution can be expanded in a series as

$$u_{aber} = \sum_{n=0}^{\infty} c_n^{*} u_{n0} = \sum_{n=0}^{\infty} c_n^{*} L_n \frac{2r^2}{w^2} u_{00} \tag{10}$$

Here, L_n are the Leguerre polynomials [3] and the coefficients c_n can be calculated using

$$c_n = 2\pi \int_0^{\infty} u_{n0}(r) u_{aber} r dr \quad . \tag{11}$$

Thus the characteristics of the beam can be determined if the τ OPL at each point is known.

3.3 THE PROGRAM

The modeling program was originally written in Matlab by Guido Mueller and Rupal Amin, to determine the properties of a beam after it passes through two lenses. We modified the code, adding a heating beam to induce a thermal lens and removing the second lens entirely. Several variables must be defined to fully describe the system. The wavelengths of the two beams, their initial waist sizes, and their inverse radii of curvature, as well as the maximum power of the heating laser, must be input. The characteristics of the Schott glass are entered in to the subroutine (Table I).

TABLE I: Characteristics of Schott glass.

Parameter	**Value**
index of refraction	1.55
absorption coefficient	10 mm^{-1}
thermal conductivity	1.4e-3 W/mmK
dn/dT	2e-5 /K
length of crystal	3 mm

The program first calculates the *q* value for each beam according to the formula

$$q = i\pi \frac{w^2}{\lambda} \quad . \tag{12}$$

The maximum power of the heating laser is divided into 21 increments, and two arrays are defined to hold the mode coefficients (c_n) at each power and in each mode (00 and BE). The thermal phase shift for each power value is calculated using a subroutine, which takes as input the *q* value of each beam, parameters of the glass, power, and the wavelengths of the lasers. The program first calculates the coefficient c_n as defined above. A variable is defined to hold the number of terms to be calculated, in order to approximate the infinite sum. The glass is divided into 200 points for which the τ OPL will be calculated. This information is held in an array, which correlates to another array that holds the position. For each point, the sum is calculated and then multiplied by the coefficient c_n to determine the τ OPL at that point.

The radius of curvature is calculated from the waist size and τ OPL from two points using simple geometry (Fig. 5).

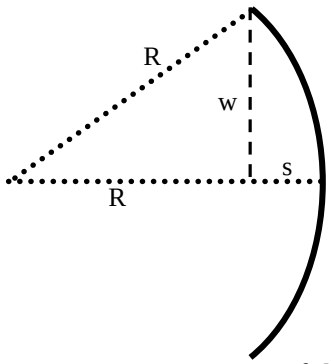

FIGURE 5: Geometry of the radius of curvature.

Using the Pythagorean theorem, we find

$$R^2 = (R-s)^2 + w^2 \tag{13}$$

which can be rearranged to find the inverse radius of curvature of the induced lens:

$$\frac{1}{R} = \frac{2s}{w^2+s^2} \quad . \tag{14}$$

Once the properties of the lens are known, the reading beam can be propagated through it as explained in the background section above. The powers in the 00 and BE modes are calculated, and returned to the main program along with the inverse radius of curvature of the reading beam.

The power itself is determined by squaring the amplitude of the beam at each heating beam power level. The final inverse radius of curvature is printed, and a graph is created plotting the power of the heating beam versus the power remaining in lower order modes, and versus the percentage of the light still mode-matched into a given cavity.

3.4 METHOD AND RESULTS

In order to explore the potential of this induced thermal lens for maintaining beam quality, the input waists of the beams were varied. The range explored for the reading beam was from 1 to 3 mm, and for the writing beam 0 to 25 mm. For each we recorded the waist sizes and the inverse radius of curvature for the reading beam, and from these calculated the minimum focal length, using the formula [4]:

$$\frac{1}{f} = \frac{n_2 - n_1}{n_1}\left(\frac{1}{R_1} - \frac{1}{R_2}\right) \quad (15)$$

Here, n_1 is the index of refraction of air and n_2 is the index of refraction of the Schott glass, while R_1 and R_2 are the radii of curvature of the two surfaces of the lens. In this experiment, the two radii are equal in magnitude but opposite in sign. The value output by the program is the inverse radius of curvature $1/R_2$. The calculated focal length for each combination of reading and writing beam sizes can be found in Table II. This modeling effort was truly a proof-of-concept test, to investigate the potential of this method for use in gravitational wave detectors, so a range of values were tested.

TABLE II: Results of model.

reading beam waist (mm)	writing beam waist (mm)	focal length (mm)
1	3	11.78
1	4	20.43
1	5	31.57
1	6	45.00
1	7	61.01
1	8	79.74
1	9	101.01
1	10	124.53
1	15	275.48
1	20	505.05
1	25	757.58
2	4	23.19
2	5	34.70
2	6	48.88
2	7	65.40
2	8	84.96
2	9	106.95
2	10	131.75
2	15	293.25
2	20	505.05
2	25	826.45
3	6	52.85
3	7	69.93
3	8	89.13
3	10	110.86
3	15	135.69
3	20	303.03
3	25	826.45

We can thus calculate the focal length of the induced lens. Our results indicate that it is possible to induce a thermal lens that has a large range in focal length. When the heating laser is off, the focal length

of the glass is infinite, and when the laser is turned on, it can be brought down to the order of meters. With an adjustment of the power of the heating laser, the focal length can be altered to the desired size.

Six representative graphs can be found in Figure 6. The title of each indicates the sizes of the reading and heating beams, both in millimeters. The top curve in each shows the fraction of the light in lower-order modes, while the bottom curve indicates the fraction of the light that is still mode-matched into a given cavity. From these graphs we can see that the power lost to higher-order modes is minimal; in most cases it is less than 10% even for the maximum power of the heating beam.

3.5 CONCLUSION

This method has great potential for adaptive mode matching. Future studies should explore all possible values of the heating and reading beams, as well as take smaller power increments to more accurately determine the lensing effects on the reading beam. One problem with the current program is that some of the outputted graphs do not start at 100% of the power in the 00 mode. This indicates a scaling problem, since we began with the assumption that the reading beam is a perfect Gaussian beam. This problem can be corrected with the addition of a constant in the determination of the radius of curvature of the induced lens. Ideally an optimization subroutine would be added that would change this constant and find the best size. Again, this was simply a proof-of-concept, and the large increase in the time to run the program that would result from this improvement was deemed excessive. Finally, this method can be tested experimentally for application in the LIGO project.

4. EXPERIMENTAL INVESTIGATION OF NEGATIVE INDUCED THERMAL LENS

4.1 INTRODUCTION

A method has been proposed by Lawrence *et al*. to compensate for thermal distortions in optical components by heating the components [5]. In our work, the effects of using a heating coil to induce a negative thermal lens were tested experimentally using a cylindrical crystal of Terbium Gallium Garnet (TGG). The basic theory remains the same as that for the positive induced lens, only instead of using a laser to heat the crystal, we used a heating coil, or "toaster." By causing the temperature on the outside of the crystal to rise, we hope to create a positive τOPL as a function of radius. This then induces a negative thermal lens that will cause the laser beam to diverge. The current through the heating coil can be varied; thus the temperature and hopefully the temperature gradient across the crystal can be changed, and the induced lens will then be adaptive. As in the theoretical model described above, the ideal lens will have a large range of focal length and will minimize power loss to higher-order modes.

FIGURE 6: Results of modeling program.

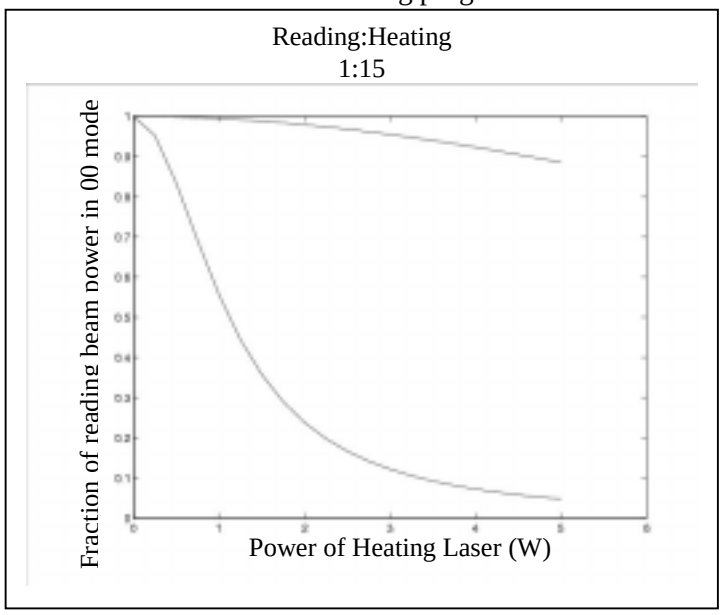

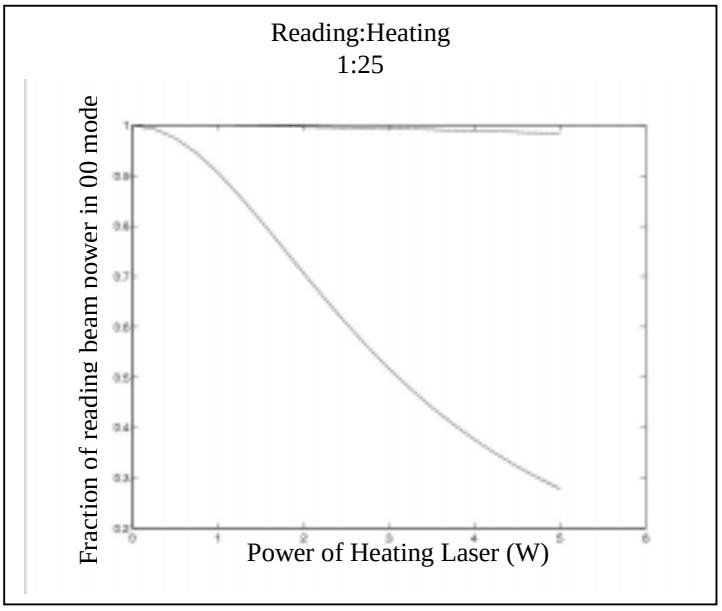

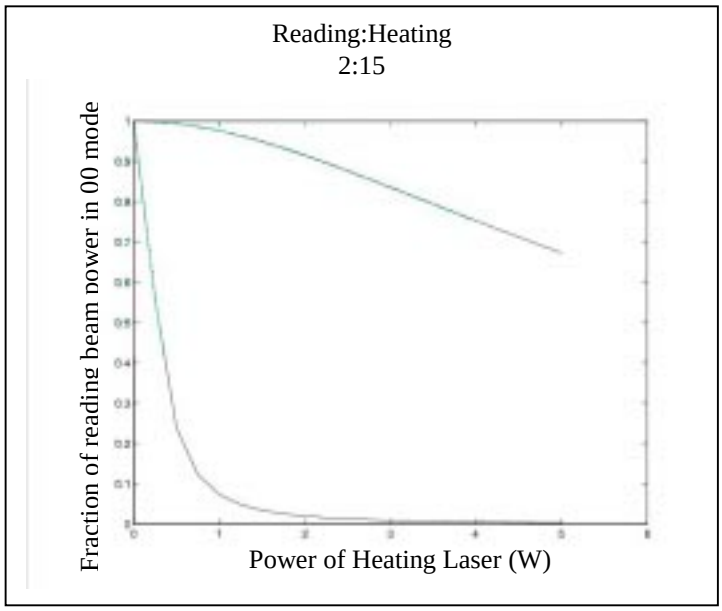

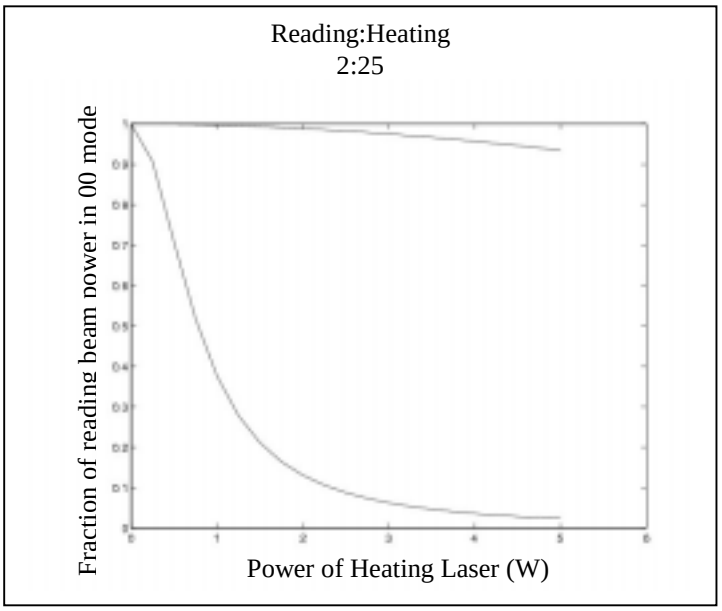

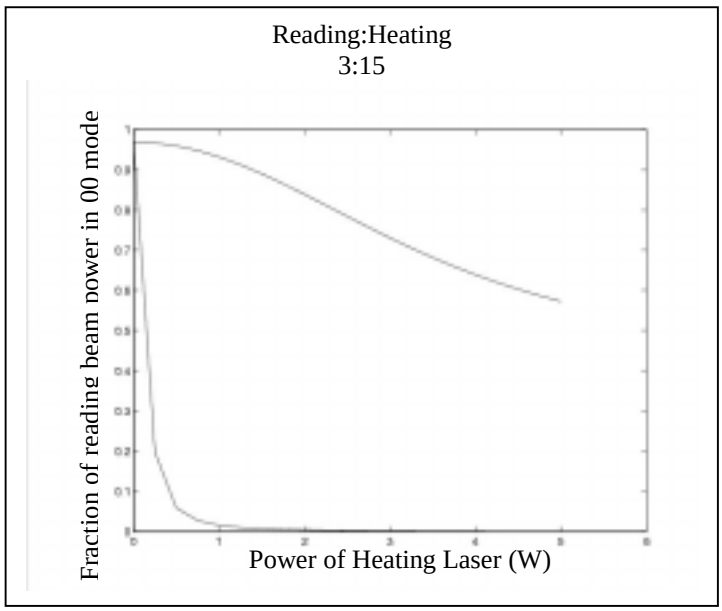

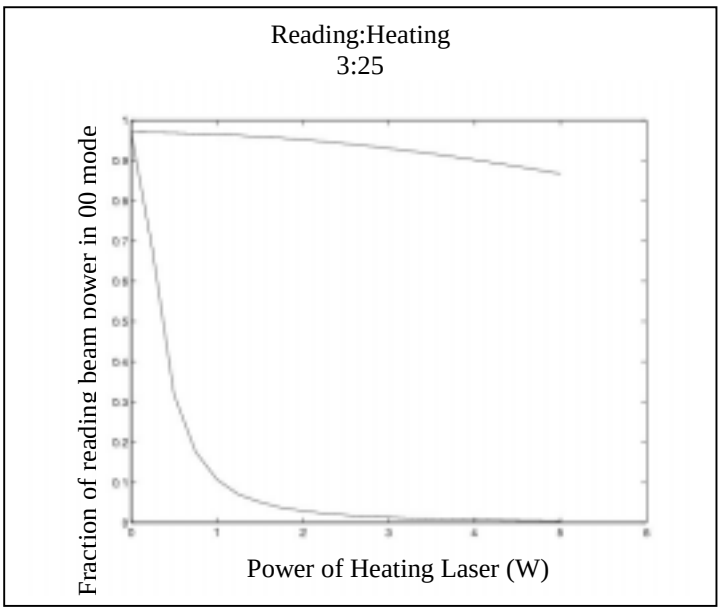

4.2 EXPERIMENTAL SETUP

The laser used was a 1064 nm YAG with 500 mW of power. A diagram of the experimental setup can be found in Figure 7. The laser first passes through a Faraday isolator, which protects the laser from back-reflections of light off the optical components. The beam then is focused and directed by a two-lens telescope and a periscope, into a fiber optic cable. This cable allows only the 00 mode through, thus cleaning the beam and allowing us to assume a perfect Gaussian beam exiting the cable. This high beam quality is important in high-accuracy applications such as gravity wave detectors. The beam is directed by a periscope into another telescope, which focuses the beam into the vacuum box containing the crystal and heating apparatus. A second periscope serves to properly align the beam into the box. Next, a three-lens telescope matches the waist size and location to that of the Fabry-Perot cavity, and two periscopes serve to align the beam with the lenses and with the cavity itself. The light that exits the cavity hits a beam-splitter. Part of the beam is focused through an attenuator into the photodiode, which is connected to the oscilloscope. The voltage registered on the oscilloscope allows us to determine the amount of power within the cavity. The remainder of the beam is focused through another attenuator into the charged coupled device (CCD) camera, connected to a dichromatic monitor, allowing us to actually see the modes that are resonating.

In LIGO, all optics are contained in a vacuum; thus for this experiment to be applicable, the crystal and the heating apparatus also had to be under vacuum. If not contained in a vacuum, the heat would be transferred through conduction by air molecules and would eventually dissipate through the walls of the box. However, under vacuum, heat can only escape through radiation, so the crystal can maintain a higher stable temperature. The TGG itself is held by two endcaps made of boron nitride, an insulating material. These support a cylindrical heat shield. Inside the shield is the heating coil itself, made of spiraled woven glass-coated Nichrome C, 22 gauge wire (0.635 mm). In order to avoid the problem of an induced magnetic field due to a current loop, the wire was folded in half and twisted together, then formed into a loop. Thus the magnetic field induced by current flowing in one direction will be canceled by current flowing in the other. A small gap was left at the top, since if the loop were completed the current would short and not run through the entire circle. Also within the heat shield are two thermocouples, one at the center of the crystal and one at the end. The entire apparatus was situated in the box parallel to the sides and centered with respect to the center of the windows in the box. Diagrams of the crystal apparatus and of the vacuum box can be found in Figure 8.

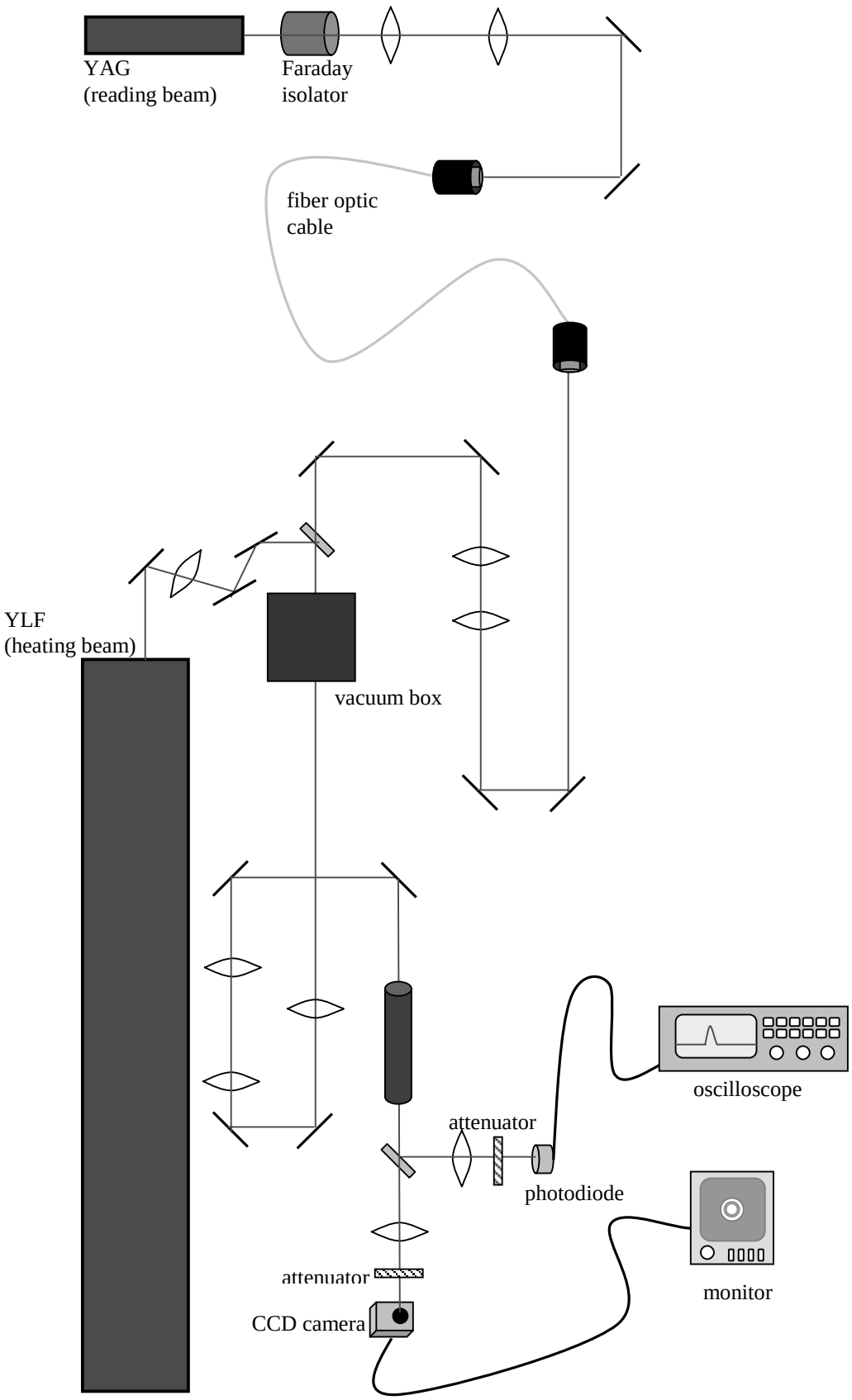

FIGURE 7: Experimental setup.

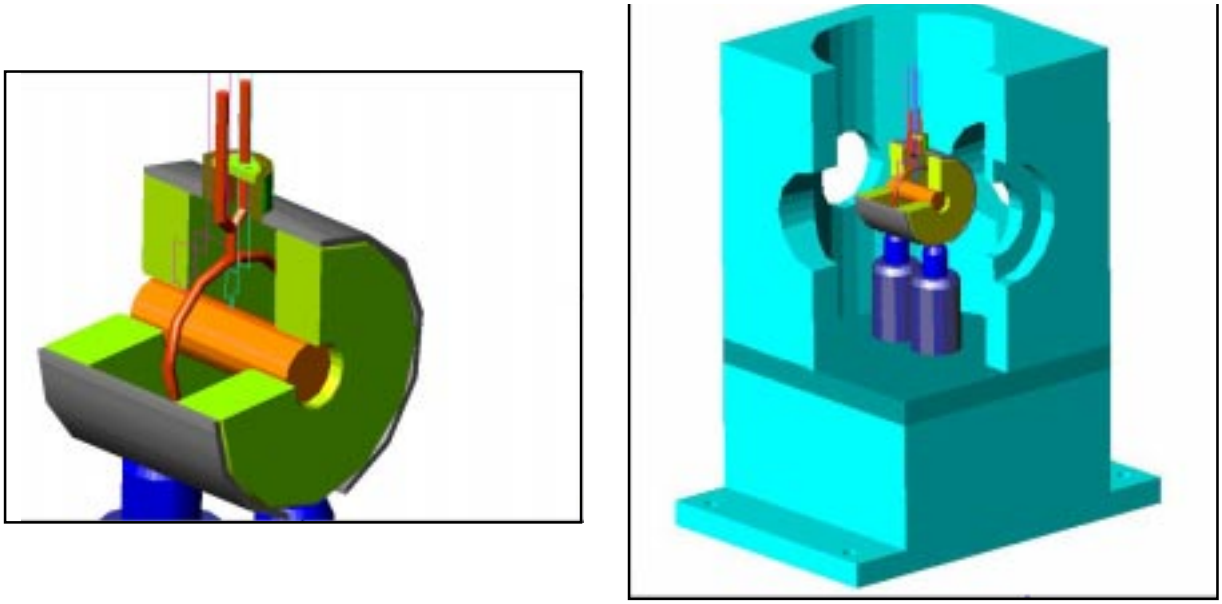

FIGURE 8: (a) Crystal apparatus and (b) vacuum box.

The vacuum box itself was modified from a previous experiment. In the existing container, there was a window on each side. In this experiment, we needed only two, so the holes parallel to the crystal were stopped with brass fittings. Glass windows were installed in the remaining holes, the first of which was anti-reflective (AR) coated. The top of the box was modified such that the four thermocouple wires and the two heating coil wires could come out, without losing the vacuum seal. The resulting apparatus was vacuum sealed and connected to a turbo vacuum pump, which reduced the gauge pressure to -100 kPa (-1 atm). This corresponds to an absolute pressure of approximately 1 kPa.

4.3 METHODS

In order for the adaptive optical element to be useful in an experimental setup, the temperature, and thus the induced lens, has to be stable. We first determined the time constant for our system. Several tests were done with the current incremented 0.33 A at a time, and the temperatures at the middle and end of the crystal were recorded approximately every 5 minutes. The temperature at any time (t) can be determined theoretically using the formula

$$T(t) = T_f - (T_f - T_i)\exp(\tfrac{t-t_0}{\tau}) \qquad (16)$$

where Ti is the temperature at t_0, T_f is the final temperature, and τ is the time constant of the system. We used the Solver function in Excel to find the final temperature and the time constant, where the initial temperature was known. The system is considered stable after three time constants. Table III shows the calculated values for the time constant, and graphs of temperature as a function of time can be found in Figure 9.

TABLE III: Time Constant Values

current (A)	τ_{end} *(min.)*	τ_{mid} *(min.)*
0 to 0.33	22.48208	23.62464
0.33 to 0.66	18.95797	15.97611
0.66 to 1	15.30172	14.85114

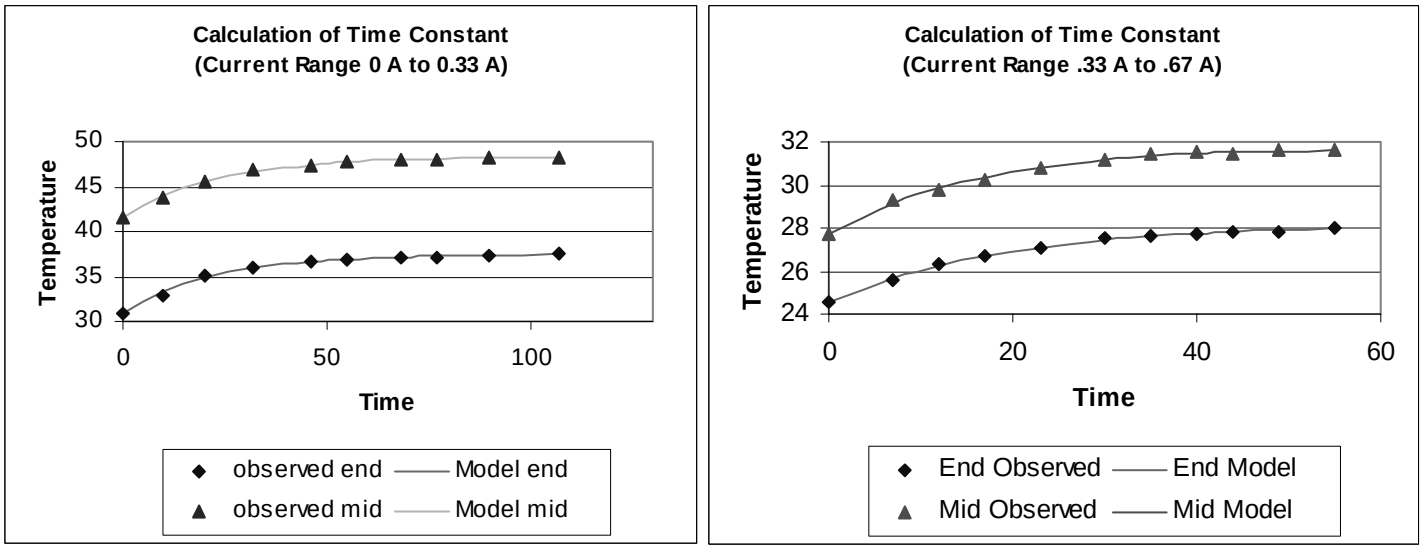

FIGURE 9: Graphs of time constant calculations.

In order to ensure the system was stabilized, the largest time constant was taken for all subsequent experiments, and each time the current was incremented, we waited one hour before taking data. Figure 10 shows a graph of final temperature as a function of current through the heating coil.

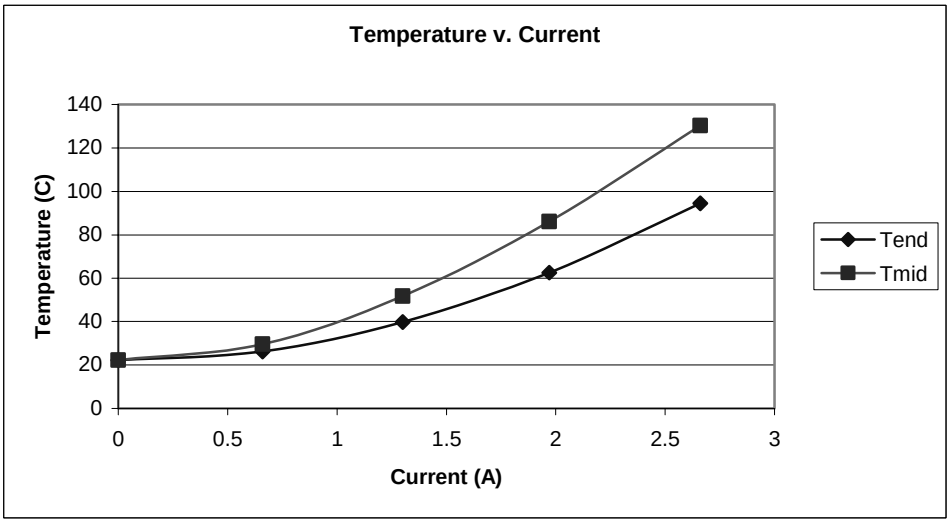

FIGURE 10: Final temperatures of the crystal.

For all the experiments performed, the same method was used. As described in the setup, an oscilloscope outputs the voltage induced by the photodiode, which is indicative of the power resonating

in the cavity. Additionally, an image of the mode can be seen on the monitor. In each case, the cavity was scanned, and the maximum voltage for each mode was recorded.

Before beginning the main experiment, we did a proof-of-concept test using an additional high power laser, the 1053 nm 50 W YLF. This is included on the diagram in Figure 7. The beam is directed by a periscope to be aligned with the YAG when it enters the vacuum box. We measured the power of the strongest modes (00, 01/tilt, and bull's eye) with the YAG laser only, the YAG and the YLF, the YAG and the toaster at 1.0 A, and all three together. Preliminary measurements indicated that the combination of the toaster heating the outside of the crystal and the YLF heating the center compensated each other, and most of the original beam quality was maintained. As far as applications to the LIGO project, this experiment was not practical. The materials used in LIGO have extremely low absorption, thus the heating due to the YLF laser is fairly excessive. However, it was useful in showing that a thermal lens is in fact induced, as shown in Table IV. The Bull's eye mode increased with the addition of the toaster and the YLF individually; however, when the two were combined, this mode decreased significantly from its power with simply the YLF. This indicates that the toaster is successful in compensating higher-order modes caused by the absorption of the YLF light.

TABLE IV: Proof of Concept for the Toaster Apparatus

	00 (mV)	***01 (mV)***	***BE (mV)***	***T_{end} (°C)***	***T_{mid} (°C)***
YAG	208	1.31	0.63	26.8	27.2
Yag and toaster (1A)	196	2.10	0.71	37.9	46.8
Yag and YLF	163	6.51	3.18	32.5	34.7
Yag, YLF, and toaster (1 A)	163	7.98	1.21	46.5	56.4

We ran the main experiment three times. In the first, a range of current from 0 A to 1.0 A corresponding to a temperature range from 27.7 to 41.8 in the middle of the crystal was increased in increments of 0.33 A. The same experiment was repeated in 0.2 A increments. The box was then realigned to ensure that the laser was properly centered on the crystal, and the current range was increased to 0 A to 2.5 A, in increments of 0.66 A. Each time three measurements were taken for each mode, and these values averaged, to minimize error. The ratio of each mode to the 00 mode was graphed versus the current. Plots showing the mode content for each experiment can be found in Figure 11. The error in these graphs is fairly significant, on the order of 10% for the weaker modes. Thus the small increases in these modes can be attributed to error, and the only mode that shows a significant change is the tilt.

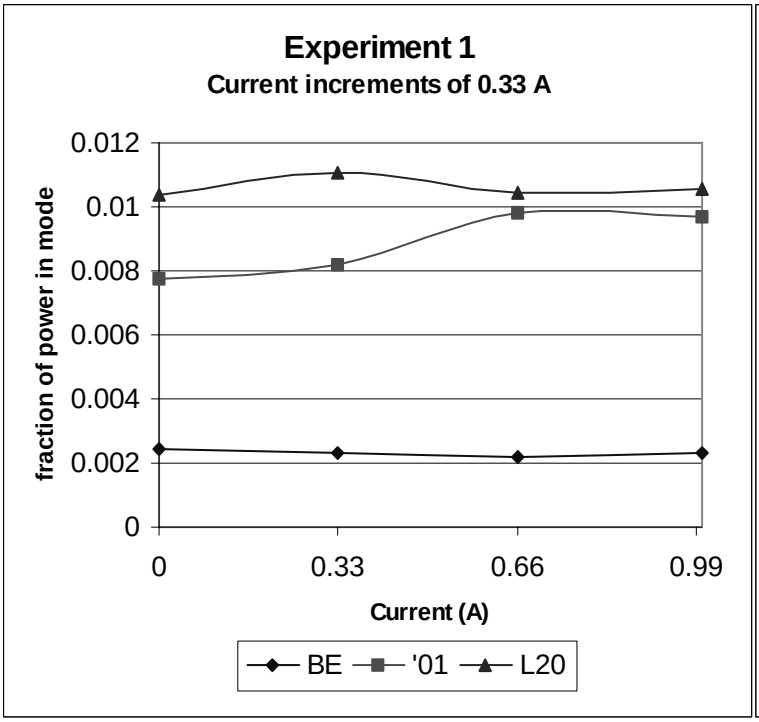

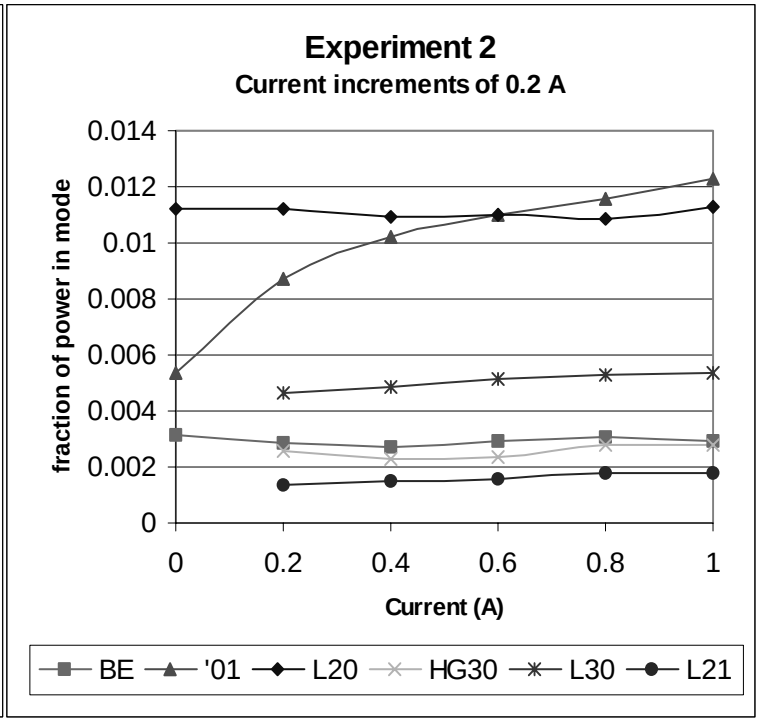

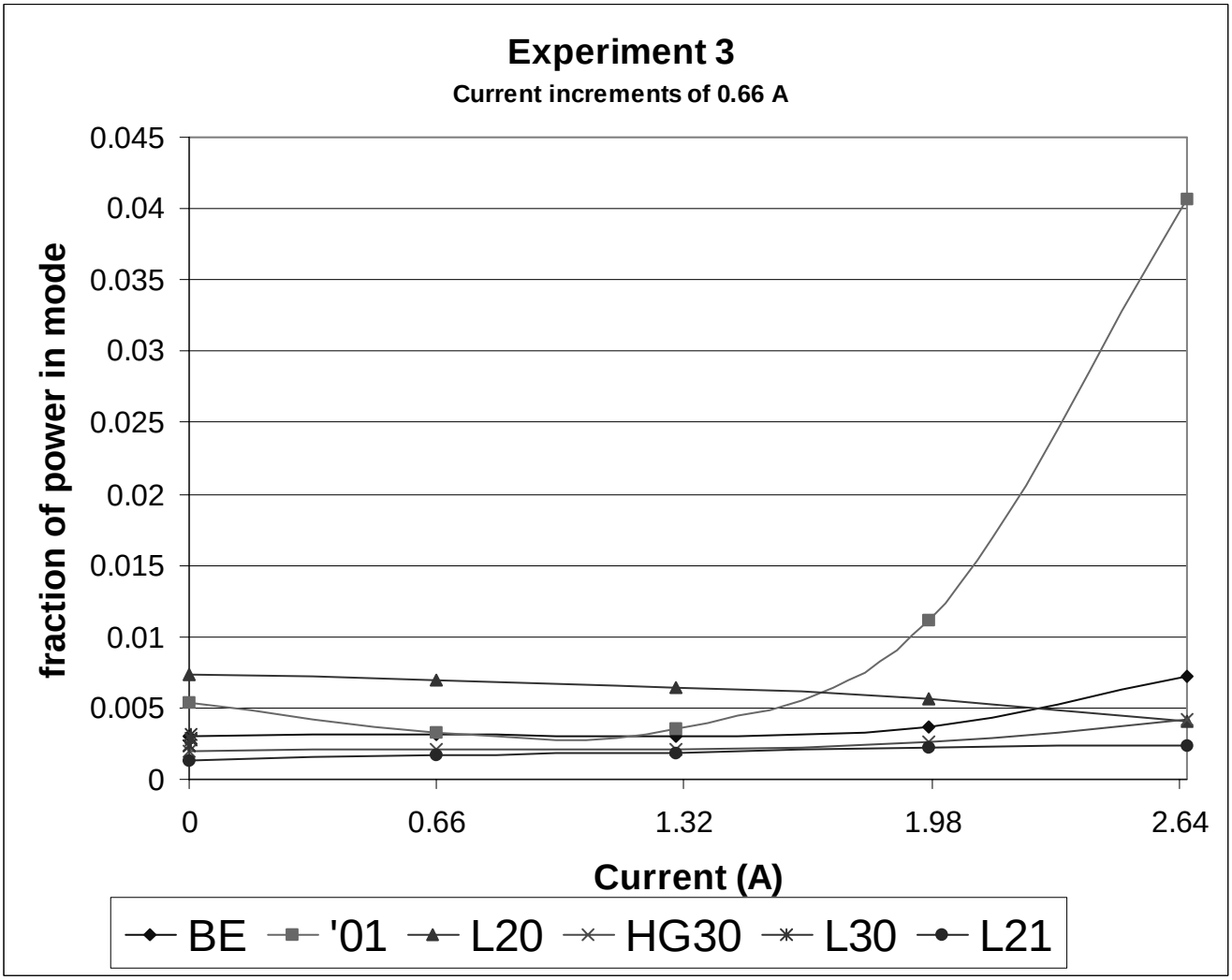

FIGURE 11: Results of three experimental runs.

4.4 RESULTS AND CONCLUSIONS

As the power was increased in each experiment, the tilt mode increased the most drastically. In the third experiment, the BE mode also increased, a common effect from a large tilt mode. The other modes remained the same within error bars. In most situations, an increasing tilt mode is indicative of a misalignment in the equipment, in our case if the laser was not hitting the end of the crystal orthogonally. However, after the second experimental run, the box was realigned, and the results from the subsequent experiments were unchanged. This indicates that something else is causing the laser to become misaligned from the cavity. The most likely candidate is uneven heating of the crystal. As described in the experimental setup of the vacuum box, the loop of Nichrome wire is not closed; an approximately 1 mm gap exists. Thus the heating of the crystal is not perfectly cylindrically symmetric. It was originally thought that the asymmetric effects would be negligible; the data indicate otherwise. In conclusion, the effects of the asymmetric heating of the crystal overshadow any effects of an induced thermal lens on the beam. However, as indicated by our initial proof-of-concept test, this does not mean that a thermal lens does not exist. In order to further explore this active compensation technique, the heating coil apparatus should be redesigned to eliminate asymmetries in the heating of the crystal. The apparatus should be very precisely aligned to ensure that the data reflect only the effects of the thermal lens.

5. CONCLUSION

Many options exist for the active compensation of thermal lensing for application in gravitational wave detectors. Two of these were explored, one theoretically and one experimentally. Both were subjected to proof-of-concept tests and showed potential in having a range of focal length while preserving beam quality. The modeling of a positive lens induced by a heating laser was very promising, and should be tested experimentally. Testing of the "toaster" method for inducing a negative lens indicated possible applications, but design modifications must be made before these can be further explored.

ACKNOWLEDGEMENTS

I would like to first thank the NSF for funding my work this summer and my advisor David Reitze for guiding me. Additionally, I would like to thank the other members of the LIGO project David Tanner, Rupal Amin, Guido Mueller, Luke Williams, Ramsey Lundock, Rachel Parks, and Wan Wu for all of their help. Finally, I would like to thank Drs. Kevin Ingersent and Alan Dorsey for making the UF REU program possible.

REFERENCES

1. A. Siegman, *Lasers* (Univ. Science Books 1986).

2. J.D. Mansell, J. Hennawi, E. K. Gustafson, M. M. Fejer, R. L. Byer, D. Clubley, S. Yoshida and D. H. Reitze. "Evaluating the effect of transmissive optic thermal lensing on laser beam quality with a Shack-Hartmann wave-front sensor," *Appl. Opt*. 40, 366-374 (2001).

3. A. Jeffery, *Handbook of Mathematical Formulars and Integrals* (Academic, London, 1995) p. 289.

4. R. L. Reese, *University Physics* (Brooks/Cole Publishing Company, California, 2000) p. 1070.

5. R. Lawrence, M. Zucker, P. Fritschel, P. Marfuta, D. Shoemaker. "Adaptive thermal compensation of test masses in advanced LIGO," Class. Quantum Grav. 19, 1803-1812 (2002).